The Nonlinear Ellipse Rotation in BK7 Glass Plate and its Application

Chunmei ZHANG, Jianliang WANG, Chuang LI, Xiaowei CHEN,

Yuxin LENG, Lihuang LIN, Ruxin LI, and Zhizhan XU

State Key Laboratory of High Field Laser Physics, Shanghai Institute of Optics and Fine Mechanics,
Chinese Academy of Sciences, P.O. Box 800-211, Shanghai 201800, China

(Received January 17, 2008)

The intensity-dependent nonlinear ellipse rotation of high-energy femtosecond pulse in BK7 glass plate is researched experimentally. The polarization, spectrum and shape of the femtosecond pulse were studied in this process. Based on this scheme, we develop a pulse temporal cleaner, which has been used in our femtosecond chirped pulse amplification (CPA) laser to provide a contrast ratio improvement of 2 orders of magnitude for the milli-joule level fs input pulses. The total transmission efficiency of the cleaner reaches 16.7%.

Key Words: Contrast, Cleaner, Glass, Nonlinear ellipse rotation, Chirped pulse amplification

1. Introduction

Chirped pulse amplification[1] (CPA) technology has made it possible to realize ultra-short and ultra-intense laser with a focused intensity as high as 10^{22}W/cm^2.[2] Then it has created exciting opportunities for the ultra-intense laser-matter interactions experiments.

Several researches about nonlinear polarization rotation(NER) have been done by other groups. The research about NER was first studied by Sala and Richardson,[3] they studied the NER in a CS2-filled cell. NER has also been studied in ordinary optical fiber[4] by Tapié and Mourou. Then Homoelle et al. studied the NER in a hollow waveguides filled with xenon.[5] The NER in air has been also studied by A.Jullien group.[6]

This paper presents the results of our research about the intensity-dependent nonlinear ellipse rotation (NER) of high-energy femtosecond pulse in BK7 glass plate. The second section summarizes the theory of NER effect. The experimental results are described and discussed in the third section.

2. Theoretical background

In this section, we give a brief introduction to the theory of optical Kerr effect and nonlinear ellipse rotation effect.[7]

2.1 Optical Kerr effect

Optical Kerr effect, generally, is the linear birefraction induced by linearly polarized laser. A linearly polarized laser pulses with enough high energy, can change the refractive index of the medium, and the change of the refractive index will influence the propagation of the laser pulses in the medium.

We suppose the frequency of the pump laser pulses (the high energy laser pulses) is ω, the polarization direction of the pump pulses is along x-axis, and the pump pulses propagate along z-axis. The detect laser (the laser beam propagating in the medium) with frequency of ω' and the polarization direction in xy-plane propagates also along the z-axis, which is parallel to the pump laser.

The nonlinear polarization in frequency ω' can be written as:

$$P_i^{(3)}(\omega') = 6\varepsilon_0 \sum_{j,k,l} \chi_{ijkl}^{(3)}(\omega' = \omega' + \omega - \omega) E_j(\omega') E_k(\omega) E_l^*(\omega)$$
$$(i, j, k, l = x, y, z) \qquad (1)$$

In isotropic medium, the third-order nonlinear susceptibility tensor $\chi_{ijkl}^{(3)}(\omega' = \omega' + \omega - \omega)$ has the following nonvanishing elements:

$$\chi_{iiii}^{(3)} = \chi_{1111}^{(3)} \qquad \chi_{iijj}^{(3)} = \chi_{1122}^{(3)}$$
$$\chi_{ijji}^{(3)} = \chi_{1221}^{(3)} \qquad \chi_{ijij}^{(3)} = \chi_{1212}^{(3)}$$
$$\chi_{iiii}^{(3)} = \chi_{iijj}^{(3)} + \chi_{ijji}^{(3)} + \chi_{ijij}^{(3)} \qquad (2)$$

So the third-order nonlinear polarization is directly obtainable from Eq.(2.1.1) and given by:

$$P_i^{(3)}(\omega') = 6\varepsilon_0 \sum_j \begin{pmatrix} \chi_{1122}^{(3)} E_i(\omega') E_j(\omega) E_j^*(\omega) \\ + \chi_{1221}^{(3)} E_j(\omega') E_j(\omega) E_i^*(\omega) \\ + \chi_{1212}^{(3)} E_j(\omega') E_i(\omega) E_j^*(\omega) \end{pmatrix}$$
$$(i, j = x, y, z) \qquad (3)$$

The nonlinear polarization along x-axis and y- axis can be described respectively as:

$$P_x^{(3)} = 6\varepsilon_0 \left(\chi_{1122}^{(3)} + \chi_{1221}^{(3)} + \chi_{1212}^{(3)}\right) \left|E_x(\omega)\right|^2 E_x(\omega')$$
$$= \varepsilon_0 \Delta\chi_{xx} E_x(\omega') \qquad (4)$$

$$P_y^{(3)} = 6\varepsilon_0 \chi_{1122}^{(3)} \left|E_y(\omega)\right|^2 E_y(\omega')$$
$$= \varepsilon_0 \Delta\chi_{yy} E_y(\omega') \qquad (5)$$

Because of $\Delta\chi_{xx} \neq \Delta\chi_{yy}$, the induced birefringence δn at ω' (i.e., the optical Kerr effect) is

$$\delta n = \Delta n_{xx} - \Delta n_{yy} = \frac{1}{2n_0}\left(\Delta\chi_{xx} - \Delta\chi_{yy}\right)$$

$$= \frac{3}{n_0}\left(\chi^{(3)}_{1212} + \chi^{(3)}_{1122}\right)\left|E(\omega)\right|^2 \quad (6)$$

Where Δn_{xx} and Δn_{yy} are the variation of the refractive index in the direction along x -axis and y - axis. The polarization direction of detect laser propagating in the medium changes by the action of optical Kerr effect.

2.2 Nonlinear ellipse rotation effect

The polarization direction of laser pulse propagating in the medium can also be changed by the optical Kerr effect induced by the laser pulse itself.

In isotropic medium, the laser pulse with frequency ω propagates along the z -axis. The third-order nonlinear polarization can be described as:

$$P_i^{(3)}(\omega) = 3\varepsilon_0 \sum_j \begin{pmatrix} \chi^{(3)}_{1122}(-\omega,\omega,\omega,-\omega)E_i(\omega)E_j(\omega)E_j^*(\omega) \\ +\chi^{(3)}_{1221}(-\omega,\omega,\omega,-\omega)E_j(\omega)E_j(\omega)E_i^*(\omega) \\ +\chi^{(3)}_{1212}(-\omega,\omega,\omega,-\omega)E_j(\omega)E_i(\omega)E_j^*(\omega) \end{pmatrix}$$
$$(i, j = x, y, z) \quad (7)$$

For convenience, we redefine the axes for the coordinate system as:

$$\vec{e}_+ = \frac{1}{\sqrt{2}}(\vec{e}_x - i\vec{e}_y) \qquad \vec{e}_- = \frac{1}{\sqrt{2}}(\vec{e}_x + i\vec{e}_y) \quad (8)$$

Here we suppose the laser beam is elliptical polarization and can be given by:

$$E(\omega) = E_+(\omega)\vec{e}_+ + E_-(\omega)\vec{e}_- \quad (9)$$

Then the third-order nonlinear polarization can change to be:

$$P_\pm^{(3)}(\omega) = \frac{1}{\sqrt{2}}(P_x(\omega) \pm P_y(\omega))$$
$$= 3\varepsilon_0 \begin{pmatrix} \left(\chi^{(3)}_{1122} + \chi^{(3)}_{1212}\right)\left|E_\pm(\omega)\right|^2 + \\ \left(\chi^{(3)}_{1122} + 2\chi^{(3)}_{1221} + \chi^{(3)}_{1212}\right)\left|E_\mp(\omega)\right|^2 \end{pmatrix} E_\pm(\omega)$$
$$= \varepsilon_0 \Delta\chi_\pm E_\pm(\omega) \quad (10)$$

The induced birefringence δn is:

$$\delta n = \Delta n_+ - \Delta n_- = \frac{1}{2n_0}(\Delta\chi_+ - \Delta\chi_-)$$
$$= -\frac{3}{n_0}\chi^{(3)}_{1221}\left(\left|E_+(\omega)\right|^2 - \left|E_-(\omega)\right|^2\right) \quad (11)$$

After the femtosecond pulse propagates distance l, the polarization axis of the femtosecond pulse rotates an angle θ is length-dependent:

$$\theta = \frac{\omega}{c}\delta n l \quad (12)$$

We can know from the Eq.2.2.5, the rotating angle θ depends to the femtosecond pulse energy.

3. Experiment and results

The experimental scheme for studying nonlinear ellipse rotation effect in BK7 glass plate is shown in Fig.1. The linearly polarized incident femtosecond pulses pass through a zero-order λ/4 waveplate to generate the elliptically polarized pulses. The angle between the polarization direction of the incident pulses and one axes of the waveplate is set as 22.5° to

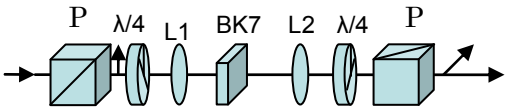

Fig.1 Experimental scheme about the nonlinear ellipse rotation effect in the BK7 glass plate. L1-L2: lenses P: polarizing beam splitter.

maximize the output efficiency. Then the femtosecond pulses are focused by an f=1.5m lens on a BK7 glass plate, which acts as a nonlinear medium for the high-intensity femtosecond pulse. In the glass plate, the polarization direction of the high-intensity part of the pulse is rotated for stronger third order nonlinear process, and the polarization direction of the other part (the weaker part) is almost unchanged for the much lower peak intensity. After the glass plate, the beam is collimated by another f=1.5m lens, and passes through another zero-order λ/4 waveplate, which fast axis is perpendicular to that of the first λ/4 waveplate. In this way, the polarization state of the low-intensity part of the femtosecond pulses returns to the initial state, but the polarization of the high-intensity portion of the pulse is rotated, just perpendicular to the polarization state of input pulse. Then the femtosecond pulses pass a polarizing beam splitter, which is used as polarization analyzer to separate the high intensity pulses from all the other components. Then, the femtosecond pulse can be pure to increase the pulse contrast by this method.

Our experiments were carried out on a commercial TSA25 CPA laser system. The laser system can output 10mJ/51fs pulses at 800nm with 10-Hz repetition rate. An energy adjuster consists of a polarizer and a 1/2 waveplate is used after the system to tune the energy of incident pulse continually. The thickness of the BK7 glass plate used is 1mm, and the glass plate is placed after the focus point. We accurately adjusted the distance between the glass plate and the second lens L2 to maximize the output efficiency by adjusting the peak intensity on the glass plate to 10^{11}W/cm^2 level.

With 2.5mJ incident femtosecond pulse, we succeeded in producing output pulse with the energy of above 0.42mJ. Thus, the total energy conversion efficiency of the whole scheme is above 16.7%. By taking into the losses from the reflections on uncoated BK7 glass plate, we can assert that the internal efficiency should be higher. In addition, the energy conversion efficiency can be increased by use of antireflection-coated glass in real application.

The pulse duration of the incident and output femtosecond pulses are measured by single-shot autocorrelator (SSA) (Shown in Fig.2). It shows the output pulse is not stretched significantly, the pulse duration keeps almost same (~50fs).

In the term of the output pulse spectrum, our scheme is more suitable for CPA laser system. A broadened spectrum with a shape of saddle can be obtained from our scheme, which is more suitable for gain narrowing effect compensation in the CPA amplification system. We will discuss why this kind of spectra is produced in the later part. The comparable spectrum curves of initial pulse and output pulse are shown in Fig.3.

We also use this scheme with lower input pulse energy as comparison. When the input energy was decreased to 1.2mJ, we succeeded in producing pulse with the energy of above 0.2mJ. Thus, the energy conversion efficiency of the setup is almost same with different input pulse energy. The pulse shape and the pulse duration have not changed also. But the

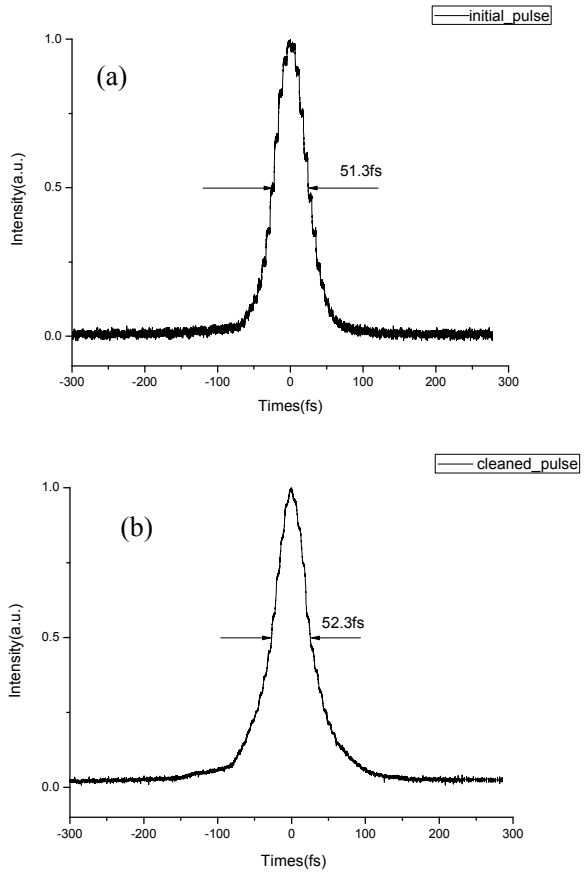

Fig.2 Normalized intensity autocorrelations of the initial pulse and output pulse. (a) initial pulse (51.3fs, FWHM). (b) output pulse (52.3fs, FWHM).

spectrum of output laser shows a shape with three peaks, and it's narrower than the initial pulse. The spectrum curves of the initial pulse and output pulse with lower input energy pulse are compared in Fig.4.

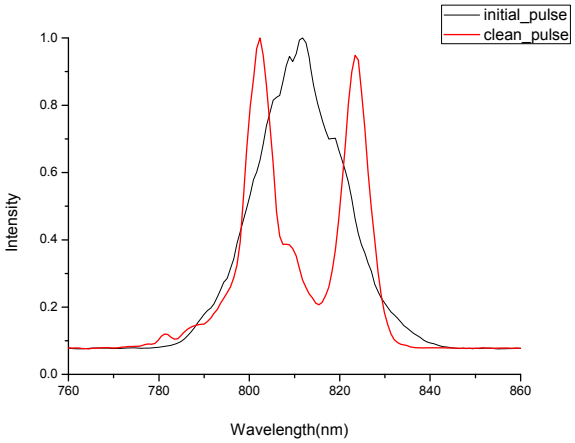

Fig.3 Comparable spectrum curves of initial pulse (black curve) and output pulse (red curve)

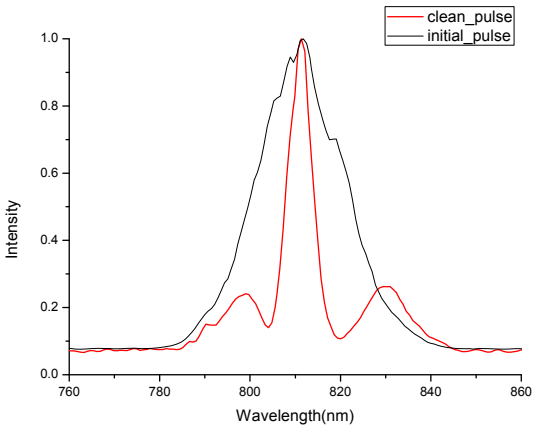

Fig.4 Comparable spectrum curves of initial pulse (black curve) and output pulse (red curve) with lower energy input pulse.

With the increase of the input pulse energy, the output pulse spectrum becomes more and more narrow, and some new spectral components begin to appear on the both sides. When the pulse energy becomes high enough, the output pulse spectrum gradually becomes a shape of deep saddle, and is broadened. The evolvement of spectrum is the result of diffraction, dispersion, SPM, and plasma behavior[8] during the propagation in medium. The output spectrum is gradually broadened with the increase of the input pulse energy, because SPM is the main mechanism to generate new spectral components during the propagation and how it strong depends on the input pulse intensity.[9] It is consistent to the result of numerical simulation in Ref10. In addition, the evolvement of pulse spectrum in two perpendicular polarization direction are the same, so that after the polarizing beam splitter, the output pulse and the leaked pulse have the same spectrum with the shape of saddle.

4. Application

Considering our scheme can separate the high-intensity portion of the pulse from the weaker part, our scheme can be used as a pulse cleaner to improve the laser contrast ratio.

The incident and output pulses are characterized by a home made third-order cross correlator shown in Fig. 5, which is based on frequency doubling and mixing with nonlinear crystals.

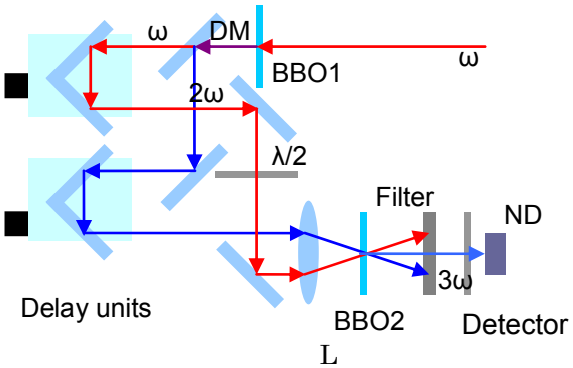

Fig.5 Setup of the home made third-order cross-correlator. BBO1, BBO2: nonlinear crystals; DM: dichroic mirror; L: lens; ND: neutral density filters.

Along the direction of the laser beam, a 0.3mm-thick type I BBO crystal is used to generate the 2ω-pulse. Then the laser beam is divided at a thin dichroic mirror. The translation stage of the ω arm, driven by a step motor, has a travel range of 10cm and the reflection stage of the 2ω arm, also driven by a step motor, has another travel range of 10cm and makes it possible to scan up to 1.33ns. The third-harmonic generation (THG) is achieved by non-collinearly wave-mixing the two beams from ω and 2ω arms at a 0.5mm-thick type I BBO crystal. We use a focusing geometry to get the strong enough energy of the 3ω signal to make measurement. Background noise scattered from ω and 2ω beams is removed using a band-pass filter at 266nm, as illustrated in Fig. 2. We have

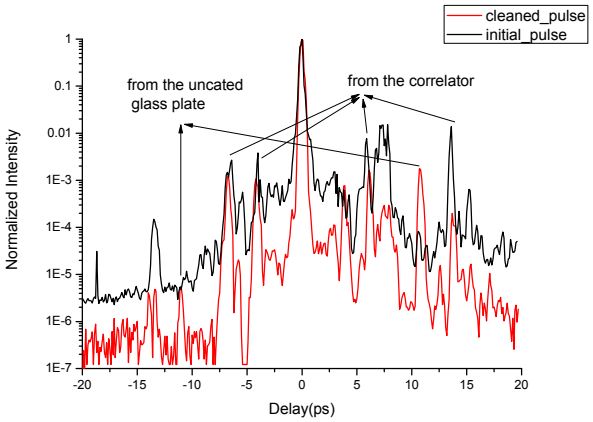

Fig.6 Third order correlation curves initial pulse (red curve) and cleaned pulse (black curve).

changed the polarization of ω arm laser from horizontal to vertical to match with 2ω arm laser in the second crystal.

We measured the contrast of the cleaned and initial pulses with the same energy. The comparable contrast curves are shown in Fig.3. For the pulse has been stretched in the process of measurement, we must consider an attenuation factor (about 5-6) of the peak level.[11] Therefore, the actual laser contrast should be higher than the results shown in Fig.6

There are two significant prepulses in -13.3ps and -18.7ps respectively before the main pulse in initial pulse, and other small pulses are brought by the third-order cross correlator. So that, the real contrast of the initial pulse is ~ 10^4 and the ASE intensity level is 5-6 orders of magnitude below the peak intensity of the main pulse. After the pulse cleaner, the contrast ratio is improved to 10^5-10^6, and the ASE intensity level is lowered above one order of magnitude. Considering our attenuation factor, the real contrast of the cleaned should be above 10^6. Limited by the correlator's dynamic range, we cannot measure the ASE pedestal level below 10^7 exactly. So we believe using our new scheme can improve the contrast 2 orders of magnitude at least.

It can be shown in Fig.3, for the prepulses with higher energy level, such as one in -13.3ps time delay, our scheme can offer a contrast ratio improvement of 2 orders of magnitude; for the prepulses with lower energy level, such as that in -18.7ps time delay, our scheme can make them obliterated completely in the background.

Our scheme, as a laser cleaner, has several advantages in efficiency, stability, configuration, pulse shape and output spectrum. First, using the glass as the cleaning medium makes the setup much simpler, without using complicated vacuum system. The simpler structure creates opportunities for broadly application. Second, for the glass is isotropic, the scheme does not need much adjustment, so the energy conversion efficiency of our scheme is stable enough, the shift of output energy is below 10%. In addition, our scheme is suitable for the pulse cleaning of higher energy laser. With 2.5mJ incident energy, the output energy is above 0.42mJ, which is almost the highest output pulse energy in pulse cleaning.

5. Conclusion

In conclusion, we researched the nonlinear ellipse rotation (NER) effect of BK7 glass plate. This scheme we set up can be used as a femtosecond laser pulse cleaner and produce a contrast improvement of 2 orders of magnitude at least for the incident pulse with higher energy. According to the limiting of our correlator's dynamic range, the real contrast improvement of our scheme maybe better. The total energy conversion efficiency of the cleaner scheme is above 16.7%. If the BK7 glass plate is AR coated, the energy conversion efficiency should be higher. Comparing to the former technologies[5),6)], this scheme can offer a number of advantages: simpler, stable conversion efficiency, no significant influence on the pulse duration, and pulse spectrum with a shape of saddle which is more suitable for gain narrowing effect compensation in the following amplification process.

Acknowledgement

This work is supported by the National Basic Research Program of China (Grant No. 2006CB806000), the Chinese National Natural Science Foundation, the Knowledge Innovation Program of the Chinese Academy of Sciences (Grant No. KGCX-YW-417-2), Shanghai Commission of Science and Technology (Grant No. 07JC14055) and Science and Technology Commission of Shanghai Municipality (Grant No. 07JC14055).

References

1) D. Strickland and G. Mourou: Opt.Commun. **56** (1985) 219.
2) M. Aoyama, K. Yamakawa, Y. Akahane, J. Ma, N. Inoue, H. Ueda, and H. Kiriyama, , Opt. Lett. **29** (2004) 2837.
3) K. Sala and M. C. Richardson, J. Appl. Phys. **49** (1978) 2268.
4) G. B. Altshuler, V. B. Karasev, S. A. Kozlov, T. A. Murina, and N. N. Rozanov, Opt. Spectrosk. **61** (1986) 359.
5) D. Homoelle, A. Gaeta, V. Yanovsky, and G. Mourou: Opt. Lett. **27** (2002) 1646.
6) A. Jullien, F. Auge-Rochereau, G. Cheriaux, J. P. Chambaret, P. d'Oliveira, T. Augusta, and F. Falcoz: Opt. Lett. 29 (2004) 2184.
7) Shen Y R.*The Principles of Nonlinear Optics* (New York: Wiley, 1984) chapter.16.
8) J.S.Liu, H. Schroeder, S.L. Chin, Ruxin Li,Wei Yu, and Zhizhan Xu, , Phys. Rev. A, **72** (2005) 053817.
9) Xiaowei Chen, Yuxin Leng, Jun Liu, Yi Zhu, Ruxin Li, Zhizhan Xu: Opt.Commun, **259** (2006) 331.
10) J.Liu, Xiaowei Chen, Jiansheng Liu, Yuxin Leng, Yi Zhu, Jun Dai, Ruxin Li, Zhizhan Xu: Acta Phys. Sin, **55** (2006) 1821.
11) K.-H. Hong, B. Hou, J.A. Nees, E. Power, G.A. Mourou: Appl. Phys. B **81** (2005) 447.